Revista Mexicana de Astronomía y Astrofísica, **47**, 63–73 (2011)

UBVR POLARIMETRY OF HIGH-GALACTIC LATITUDE CARBON STARS

J. M. López and D. Hiriart

Instituto de Astronomía
Universidad Nacional Autónoma de México, Ensenada, B. C., Mexico

Received 2010 October 20; accepted 2011 January 17

RESUMEN

Presentamos polarimetría y fotometría en las bandas *UBVR*, en el periodo de un año, de ocho estrellas de carbón de alta latitud galáctica: V Hya, CZ Hya, R For, R Lep, Y Cvn, T Dra, RV Aqr y RT Cap. La polarización observada alcanza su máximo valor en la banda U y es muy variable en el tiempo. Similarmente, la polarización en la banda B es muy variable pero sus valores son siempre inferiores a los obtenidos en la banda U. El origen y la variabilidad de la polarización en estas bandas puede explicarse como el resultado de la dispersión de la radiación de la estrella central en las regiones interiores de la envolvente circunestelar donde los granos de polvo y las moléculas son creados, destruidos y mezclados por ondas de choque.

ABSTRACT

We present *UBVR* polarimetry and photometry obtained over a period of one year of eight high-galactic latitude carbon stars: V Hya, CZ Hya, R For, R Lep, Y Cvn, T Dra, RV Aqr, and RT Cap. The observed polarization is highest in the U band and highly variable with time. Similarly, the polarization in the B band is highly variable but the values are always lower than those in the U band. The origin and variability of the linear polarization in these bands may be explained as dispersion of radiation from the central star at the inner regions of the circumstellar envelope, where grains and molecules are created, destroyed, and stirred by shock waves.

Key Words: circumstellar matter — polarization — stars: carbon — stars: variables: general

1. INTRODUCTION

It is known that some evolved stars present circumstellar envelopes of dust and gas. These envelopes are the result of mass loss from the star driven by a strong wind. The spectral energy distribution emerging from the circumstellar envelope presents a double peak with the one at the longest wavelength produced by dust emission. Also, some of these stars have strong emission of molecular lines associated with the envelope.

The geometry of these envelopes is a fundamental parameter assumed to be responsible for the observed morphologies of planetary nebulae (Johnson & Jones 1991; Trammell, Dinerstein, & Goodrich 1994). Some models used to reproduce the observed morphologies in planetary nebulae take into account the geometry of the original circumstellar envelope (Kahn & West 1985; Habing, te Lintel Hekkert, & van der Veen 1989).

Circumstellar envelopes are usually not resolved. Therefore photometry is not an appropriate technique to study their morphology since it is not possible to determine their evolution by photometric monitoring over the medium to long term, because a change in the shape of the envelope does not necessarily imply a variation in the integrated flux of the object. Polarimetry is the proper technique to study their morphology since modifications in the geometry may be related to variations in the position angle of the polarization vector.

Starlight is not polarized due to the thermal nature of the radiation. However, an evolved star surrounded by an envelope will produce a certain amount of polarization if the shape of the envelope

TABLE 1

BASIC DATA OF THE PROGRAM STAR

Star	Variability Type	Galactic longitude $l^{II}(^\circ)$	Galactic latitude $b^{II}(^\circ)$	Spectral Type	Period (days)
V Hya	SRa	269	+33.6	C7.5,E	531
CZ Hya	Mira	266	+29.9	Nev,C	442
R For	Mira	215	−68.1	C0,E	389
R Lep	Mira	214	−31.3	C7,6E	430
Y Cvn	SRb	126	+71.6	C7,I	157
T Dra	Mira	86	+29.9	N0,E	422
RV Aqr	Mira	49	−29.6	C0,E	454
RT Cap	SRb	22	−27.9	C6,II	393

departs from spherical symmetry (Trammell et al. 1994). Polarimetric monitoring of evolved stars will provide us with information about their evolution because the degree of polarization and the polarization position angle are related to changes in their morphology. Evolved stars are variables, but flux variations do not necessarily imply changes in the degree of polarization of its envelope. At low polarization values, the observations might be contaminated by interstellar polarization. The contribution of this effect is enhanced towards the galactic disc and decreases with galactic latitude.

There are strong reasons to believe that the main mechanism for polarization of stellar flux from these envelopes is light dispersion, either by dust grains ($\propto \lambda^{-1}$) or molecules ($\propto \lambda^{-4}$) formed in the cold envelope. Multi-wavelength polarimetry observations could provide us with better information to determine which of these mechanisms dominates according to its wavelength dependence. Also, a polarimetric study can give us information on the size and chemical composition of the dust grains, since polarization is a function of the refractive index.

In this paper we present *UBVR* polarimetry and photometry for a sample of eight high-galactic latitude evolved carbon stars over a period of one year. The wavelength and time dependence of their degree of polarization, the position angles, and brightnesses are presented. Four of the objects have no previously reported values for these parameters. All but one of the objects have no previously reported polarization measurements in the U band.

2. OBSERVATIONS

The basic data for the observed carbon stars are listed in Table 1. They were selected from the list of Hiriart & Kwan (2000) and Hiriart (1998) where model results for gas and dust emission from their circumstellar envelopes are available. All the selected objects have galactic latitude $|b^{II}| \geq 20^\circ$ to minimize contamination by polarization from the galactic plane. The envelopes of these stars are optically thin so they can be observed at optical wavelengths. All the stars have been observed in the infrared and molecular gas emission, from which the mass loss rates have been determined (Oloffson et al. 1993).

Linear polarization measurements were made at the 0.84 m, f/15, telescope of the Observatorio Astronómico Nacional in the Sierra de San Pedro Mártir, Mexico, using a CCD camera and the POLIMA polarimeter (Hiriart et al. 2005). The CCD camera employed an e2V chip with 2048×2048 pixels and a 13 μm pixel size, which provides a plate scale of 0.44 arc-sec pixel^{-1}. POLIMA consists of a rotating Glan-Taylor prism driven by a step motor. Since the polarimeter is a single-beam device with a very slow modulation, photometric conditions are required for accurate polarimetry. The U, B, V, and R measurements were obtained between January and December 2009 at or near the new moon phase in all cases. Only data from photometric nights were considered.

Separate images were obtained for all four wavelengths and at relative position angles of the prism of 0°, 45°, 90°, and 135°. The zero position angle was established from observations of polarized standards and it was found to be $(-91 \pm 2)^\circ$. The instrumental polarization was determined by observing unpolarized standard stars and it was found to be $(0.6 \pm 0.5)\%$. The error quoted for the instrumental polarization is relatively high because single-beam polarization measurements are affected by sky variations during data acquisition at the four position angles of the prism. We used polarized and unpolar-

ized standard stars from Schmidt, Elston, & Lupie (1992).

Data were reduced using IRAF tasks. Observations of nearby blank sky were obtained at different prism orientations using the same on-chip exposures times as for the on-source observation. Dark-current frames were not taken because of the low noise of the detector. Flat fields were taken at the four positions of the polarizer and for all the filters at dusk and dawn. Bias frames were also taken at the middle of the night. For each filter and prism position, bias frames were subtracted from the flat field images; the flat field images corrected for bias were combined to form an average flat field for each filter and prism position. The bias frame was also subtracted from each object image and the resulting frames were multiplied by the mean value of the combined bias-corrected flats. Finally, the object image was divided by the combined flat field.

The flux of the object may be determined from two orthogonal measurements $f_1 = f(0°) + f(90°)$ and $f_2 = f(45°) + f(135°)$ where $f(\theta)$ is the flux of the object at image taken at polarizer position θ. The instrumental flux is the average of these two fluxes, from which instrumental magnitudes for each object were obtained. A number of photometric standard stars were observed to determine the photometric zero points. The conversion to standard magnitudes was made using the standard photometric stars from Landolt (1992).

We calculated the normalized Stokes parameters q and u for each object as

$$q = \frac{f(0°) - f(90°)}{f(0°) + f(90°)}\,, \tag{1}$$

and

$$u = \frac{f(45°) - f(135°)}{f(45°) + f(135°)}\,. \tag{2}$$

The q and u parameters are related to the fractional polarization p and the position angle of polarization θ by

$$p = \sqrt{q^2 + u^2}\,, \tag{3}$$

and

$$\theta = \frac{1}{2}\arctan\left(\frac{u}{q}\right)\,. \tag{4}$$

By defining the fractional polarization in this way, we are assuming that the circular polarization is negligible.

2.1. *Error calculations*

The uncertainty of the flux measurement of the star is given by

$$\sigma_f = \sqrt{f_{\rm star} + 2f_{\rm sky}}\,, \tag{5}$$

where $f_{\rm star}$ and $f_{\rm sky}$ are the fluxes from the star and sky from the same image, respectively.

From equations (1) and (2), we use Gaussian propagation to obtain the errors for u and q

$$\sigma_u = \sqrt{\left[\frac{2f_{135}}{(f_{45}+f_{135})^2}\sigma_{f_{45}}\right]^2 + \left[\frac{2f_{45}}{(f_{45}+f_{135})^2}\sigma_{f_{135}}\right]^2}\,, \tag{6}$$

and

$$\sigma_q = \sqrt{\left[\frac{2f_{90}}{(f_0+f_{90})^2}\sigma_{f_0}\right]^2 + \left[\frac{2f_0}{(f_0+f_{90})^2}\sigma_{f_{90}}\right]^2}\,, \tag{7}$$

where σ_f is the error in the flux and f_x is the flux at orientation x of the polarization analyzer.

Similarly, the errors in the polarization degree, ϵ_P, and polarization position angle, ϵ_θ, follow from equations (3) and (4). Using Gaussian propagation we get

$$\epsilon_P = \sqrt{\sigma_u^2 + \sigma_q^2}\,, \tag{8}$$

and

$$\epsilon_\theta = \frac{1}{2p}\sqrt{(q\sigma_u)^2 + (u\sigma_q)^2}\,, \tag{9}$$

where σ_u y σ_q are given by equations (6) and (7), respectively, and p is the measured polarization.

3. RESULTS AND ANALYSIS

The observed polarization values are shown in Table 2. For each object, this table shows: the Julian date; linear polarization, p; position angle, θ, and errors of the measurements of p and θ (ϵ_p and ϵ_θ, respectively). Except for V Hya, all the stars were observed on more than one night.

For each star two total fluxes, f_1 and f_2, can be derived from the measurements from a couple of object images separated by 90 degrees of the polarizer prism: $f_1 = f(0°) + f(90°)$ and $f_2 = f(45°) + f(135°)$. The difference between these two fluxes expressed in percent, Dif(%), is also shown in Table 2. A low value of Dif(%) indicates sky stability during the observations assuming that star flux does not change during the observing time.

The values of p and θ as a function of wavelength are plotted from Figures 1 to 8 for each object. The polarization measurements in the U band, in general, have large errors because of the low photon flux in this band. The results of polarization measurements for each object are described in the following sections, and comparisons with previously published results are made whenever possible. A summary of these comparisons is presented in Table 3.

TABLE 2

UBVR POLARIMETRY AND PHOTOMETRY OF CARBON STARS

Name	JD (2450000.00+)	Filter	Magnitude	Dif (%)	$p \pm \epsilon_p$ (%)	$\theta \pm \epsilon_\theta$ (deg)
V Hya	4951.64	*U*	14.15±0.02	1.53	5.7±0.3	59±1
		B	12.83±0.01	0.11	3.6±0.1	59±1
		V	8.25±0.01	0.81	2.2±0.1	124±1
		R	6.02±0.01	0.07	2.8±0.1	134±1
CZ Hya	4860.97	*B*	16.14±0.02	0.28	5.0±0.5	57±2
		V	11.57±0.02	0.21	2.1±0.2	139±2
	4891.89	*B*	15.33±0.02	1.25	4.8±0.3	53±1
		V	11.00±0.02	0.37	3.2±0.1	47±1
	4913.74	*B*	14.10±0.01	1.73	8.1±0.1	78±1
		V	10.44±0.01	0.92	4.4±0.1	58±1
		R	8.81±0.01	1.05	3.0±0.1	126±1
	4952.73	*U*	15.70±0.02	0.63	10.1±0.6	49±1
		B	12.85±0.01	0.24	2.2±0.1	131±1
		V	9.71±0.01	0.01	1.4±0.1	123±1
		R	8.21±0.01	0.29	1.1±0.1	114±1
R For	4855.66	*B*	14.70±0.02	0.50	0.9±0.3	94±6
		V	10.01±0.02	0.25	0.3±0.2	77±10
	5099.91	*B*	14.17±0.02	0.15	0.4±0.1	64±7
		V	9.32±0.02	0.10	1.7±0.1	54±1
		R	7.25±0.02	0.30	2.9±0.1	60±1
	5126.82	*U*	15.35±0.02	0.72	6.0±0.5	83±2
		B	13.55±0.01	0.01	0.2±0.2	136±20
		V	8.93±0.01	0.35	2.0±0.1	61±1
		R	7.04±0.01	0.30	2.9±0.1	60±1
	5155.69	*U*	15.42±0.02	1.30	2.3±0.6	94±5
		B	13.51±0.01	0.12	0.8±0.2	75±4
		V	8.93±0.01	0.06	2.1±0.1	71±1
		R	3.00±0.01	0.08	3.0±0.1	68±1
R Lep	4860.73	*U*	12.53±0.04	1.47	4.7±0.5	102±2
		B	11.62±0.02	0.15	0.7±0.3	62±7
		V	6.98±0.02	0.58	0.8±0.2	101±4
	4891.69	*U*	12.80±0.04	1.38	3.1±0.5	55±4
		B	12.06±0.02	1.02	2.5±0.5	42±4
		V	7.34±0.02	0.03	1.7±0.2	48±2
	5067.97	*B*	14.88±0.02	0.20	2.3±0.3	76±2
		V	10.20±0.01	0.23	1.8±0.1	70±1
		R	7.70±0.01	0.05	2.8±0.1	49±1
	5155.87	*U*	14.11±0.02	0.73	5.9±0.4	102±1
		B	12.60±0.01	0.02	1.0±0.1	109±3
		V	7.70±0.01	0.20	1.0±0.1	134±2
		R	5.56±0.01	0.58	1.3±0.1	135±1
Y Cvn	4856.02	*U*	12.12±0.04	0.30	8.1±0.4	93±1
		B	8.12±0.02	0.45	0.2±0.1	103±12
		V	5.01±0.02	0.24	0.6±0.1	61±4
	4891.95	*U*	11.71±0.04	0.17	4.0±0.3	65±1
		B	8.11±0.02	0.24	0.5±0.1	102±5
		V	4.99±0.02	0.08	0.5±0.1	93±3
	4913.83	*U*	12.82±0.01	0.23	0.8±0.2	64±5
		B	7.94±0.01	0.22	1.2±0.1	115±1
		V	5.01±0.01	0.08	1.3±0.1	98±1
		R	3.64±0.01	0.28	1.6±0.1	131±1
	4925.74	*U*	12.81±0.01	0.19	1.3±0.2	48±4
		B	7.87±0.01	0.25	0.8±0.1	50±2
		V	4.97±0.01	0.88	1.5±0.1	49±1
	5001.72	*U*	12.83±0.01	1.37	5.1±0.2	97±1
		B	8.06±0.01	0.35	0.6±0.1	138±3
		V	5.06±0.01	0.06	0.7±0.1	92±3
		R	3.47±0.01	0.48	1.7±0.1	75±1

TABLE 2 (CONTINUED)

Name	JD (2450000.00+)	Filter	Magnitude	Dif (%)	$p \pm \epsilon_p$ (%)	$\theta \pm \epsilon_\theta$ (deg)
T Dra	4913.93	*B*	13.86±0.01	0.71	4.4±0.1	95±3
		V	9.67±0.01	0.41	2.6±0.1	106±1
		R	7.94±0.01	0.18	2.3±0.1	104±1
	4951.88	*U*	16.17±0.02	1.91	5.7±0.7	113±3
		B	13.21±0.08	0.09	4.0±0.2	112±1
		V	9.24±0.01	0.02	3.5±0.1	100±1
		R	7.59±0.01	0.36	2.4±0.1	104±1
	5000.77	*U*	16.21±0.02	0.27	2.3±0.7	102±7
		B	13.30±0.01	0.40	6.1±0.1	116±3
		V	9.40±0.01	0.01	3.5±0.1	108±1
		R	7.64±0.01	0.27	3.2±0.1	103±1
	5039.72	*U*	16.33±0.03	0.29	8.2±0.8	114±1
		B	13.76±0.01	0.59	6.5±0.2	116±1
		V	9.78±0.01	0.16	3.8±0.1	117±1
		R	7.91±0.01	0.02	2.7±0.1	108±1
	5067.69	*U*	16.59±0.04	1.05	7.2±0.8	100±2
		B	14.17±0.02	0.12	4.2±0.2	113±3
		V	10.19±0.01	0.17	3.6±0.1	114±1
		R	8.11±0.01	0.09	2.4±0.1	109±1
RV Aqr	5000.97	*V*	11.65±0.01	0.05	7.41±0.31	106±1
		R	9.41±0.01	0.16	5.18±0.18	114±1
	5038.87	*B*	16.94±0.01	0.75	8.22±0.49	107±1
		V	12.13±0.01	0.17	7.81±0.19	111±1
		R	9.73±0.01	0.12	6.22±0.12	113±1
	5096.64	*B*	17.51±0.02	0.68	7.68±0.49	115±1
		V	12.45±0.02	0.02	7.36±0.16	114±1
		R	9.90±0.02	0.16	6.22±0.11	120±1
	5126.63	*B*	16.98±0.02	0.07	5.67±0.45	120±2
		V	12.11±0.01	0.15	6.66±0.19	117±1
		R	9.75±0.01	0.51	6.47±0.12	121±1
RT Cap	5003.9	*U*	14.06±0.02	1.60	4.14±0.48	106±2
		B	10.80±0.01	0.43	1.23±0.13	107±2
		V	6.93±0.01	0.01	2.24±0.09	88±1
		R	5.27±0.01	0.54	2.69±0.08	107±1
	5038.85	*U*	13.89±0.03	0.29	3.61±0.40	105±2
		B	10.40±0.01	0.07	1.47±0.13	100±2
		V	6.78±0.01	0.37	1.11±0.10	135±2
		R	5.11±0.01	2.19	3.64±0.13	102±1
	5067.76	*U*	14.17±0.03	0.09	9.90±0.36	91±1
		B	10.63±0.02	0.04	1.84±0.12	89±1
		V	7.05±0.01	0.40	1.04±0.11	107±2
		R	5.22±0.01	0.13	1.81±0.13	92±1
	5095.63	*U*	14.55±0.03	2.15	5.40±0.32	112±1
		B	11.07±0.02	0.13	0.46±0.11	134±5
		V	7.07±0.02	0.11	1.13±0.09	109±2
		R	5.55±0.02	0.49	1.74±0.12	77±1
	5127.58	*U*	14.34±0.02	0.32	5.14±0.43	105±2
		B	11.33±0.01	0.22	1.74±0.17	98±2
		V	7.61±0.01	0.24	1.85±0.10	92±1
		R	5.63±0.01	0.65	1.61±0.10	78±1

3.1. *V Hya*

Figure 1 shows the polarization and position angle of V Hya in the *UBVR* bands. This star was observed only once at JD=2454951.64. Spectropolarimetry of V Hya was performed by Trammell et al. (1994) in the range of $\lambda\lambda 5000 - 7000$, who obtained an average polarization of 3.01 ± 0.01 and $10.06 \pm 0.05\%$ at position angles of $124 \pm 1^\circ$ and $94 \pm 1^\circ$ for April 1992 and January 1993, respectively. The ranges of these values are in agreement with the ones presented in this work. Kruszewski, Gehrels, & Serkowski (1968) report polarization in the *B* filter of 2.73 to 3.17% over a span of 169 days, while the polarization in the yellow filter varied from 1.78 to 2.25% over the same period of time. Serkowski & Shawl (2001) obtain values of the degree of polarization in the following ranges for each filter: $U =$ (1.52 to 1.66)% during 76 days; $B =$ (1.31, 3.14)%

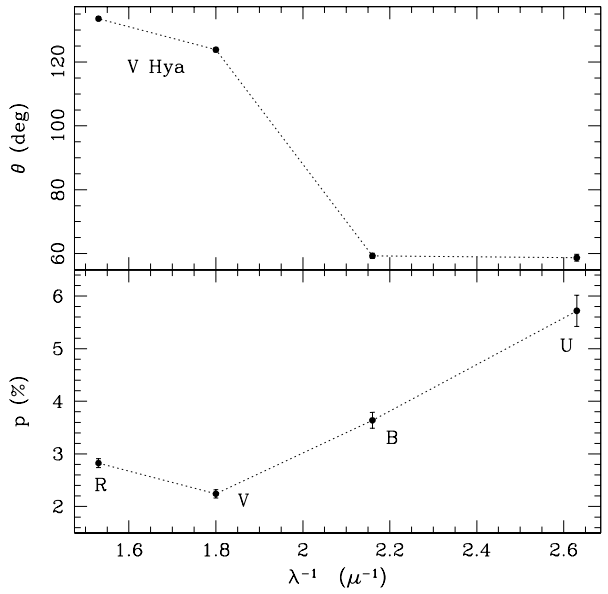

Fig. 1. Polarimetric observations of V Hya obtained on JD=2454951.64 for degree of polarization (lower panel) and position angle (upper panel) as a function of wavelength.

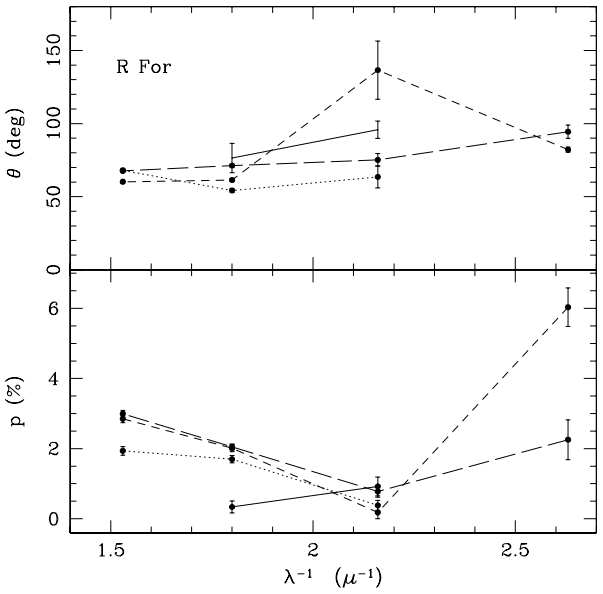

Fig. 2. Same as Figure 1, but for R For on JD=2454855.66 (solid line), 2455099.91 (dotted line), 2455126.82 (short-dashed line), and 2455155.69 (long-dashed line).

over 12,517 days; $V = (0.68, 2.26)\%$ for a period extending from JD=2439499 to 24352016. Our polarization value in the U band, 5.7%, is much higher than theirs, but their polarization values in the B and V bands are similar to the ones we find.

3.2. *R For*

Polarization observations of R For in the U and B bands by Serkowski & Shawl (2001) show values of $1.95 \pm 1.64\%$ and $0.92 \pm 0.2\%$ with position angles of 121° and 172°, respectively, for JD=2439500. For the U band we obtained a polarization of $6.0 \pm 0.5\%$ on JD=2455126.82, and $2.3 \pm 0.6\%$ on JD=24455155.69, with a polarization position angle of 82° and 94°, respectively. Our U polarization values are higher than those reported by Serkowski & Shawl (2001). Our values for the polarization in the B band are in the range of 0.18 to 0.923% with position angles in the range of 63 to 136° which are consistent with the ones reported by Serkowski & Shawl (2001).

3.3. *R Lep*

Polarimetric observations of R Lep extend back for 40 years (Kruszewski et al. 1968; Serkowski 1971; Dyck & Sandford 1971; Raveendran & Kameswara Rao 1989; Serkowski & Shawl 2001; Raveendran 2002). All the reported B and V polarization values are in agreement with the data presented in this paper. Our U-band measurements are the first published for this object.

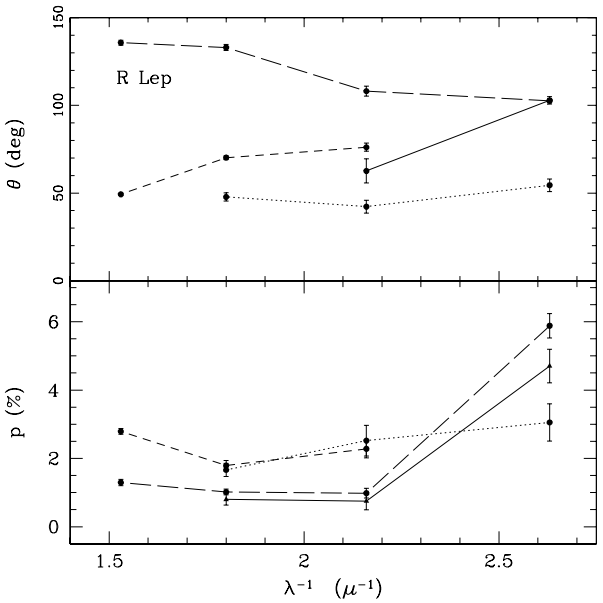

Fig. 3. Same as Figure 1, but for R Lep on JD=2454860.73 (solid line), 2454891.69 (dotted line), 2455067.97 (short-dashed line), and 2455155.87 (long-dashed line).

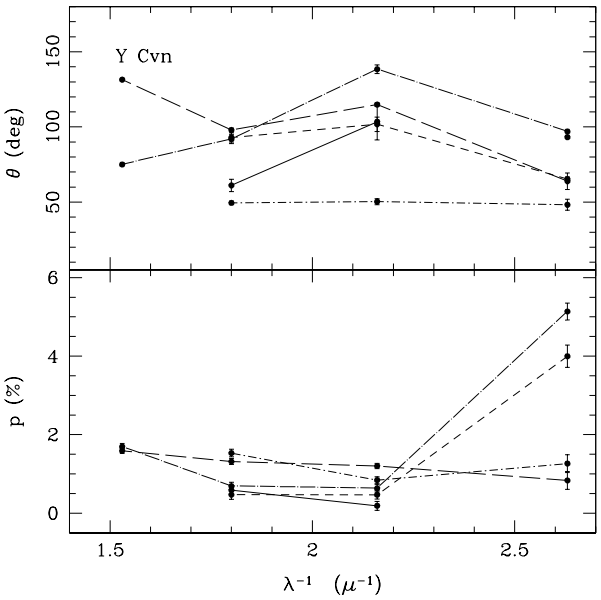

Fig. 4. Same as Figure 1, but for Y Cvn on JD=4856.02 (solid line), 4891.95 (dotted line), 4913.83 (short-dashed line), 4952.74 (long-dashed line), and 5001.72 (dot short-dashed line).

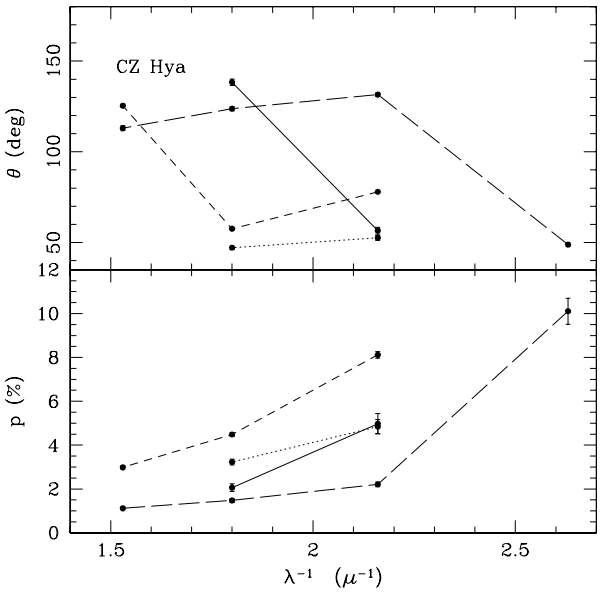

Fig. 5. Same as Figure 1, but for CZ Hya on JD=2454860.97 (solid line), 2454891.89 (dotted line), 2454913.74 (short-dashed line), and 2454952.73 (long-dashed line).

Raveendran (2002) presents polarimetry for R Lep in the *BVR* bands during 1991–2002 when the star went through an episode of fading brightness at light maximum after an interval of 3 yr. The percentage of linear polarization increased as the fading progressed and attained a maximum of 3% in the *V* band, close to the minimum; it remained more or less at the same level during and well after the star returned to normal brightness. Raveendran suggests that the physical mechanism that causes the rather large polarization is perhaps selective extinction by aligned foreground grains produced by the passage of shock waves through the circumstellar envelope.

3.4. *Y Cvn*

Raveendran (1991) carried out polarimetric observations of Y Cvn close to a light maximum and obtained values close to zero in the *BVRI* bands on JD=2446117.48. Serkowski (1971) reported a value of ∼0.25% for Y Cvn in the blue region. We have found a polarization of about ∼1.0% in the *BVR* bands and a relatively high and variable polarization in the *U* band for this star. Y Cvn is a high galactic latitude object ($b^{\rm II} = 72°$). The low polarization listed in Table 2 for the *BVR* bands indicates that the interstellar component of the polarization is almost zero.

3.5. *Other objects*

As far as we know, our polarization measurements are the first for the remaining objects: CZ Hya, T Dra, RV Aqr, and RT Cap.

4. DISCUSSION

4.1. *Wavelength dependence of polarization*

Even though the emission from evolved carbon stars is relatively dim at short wavelengths, we were able to measure linear polarization in the *B* and *U* bands. When both were measured for each object, the highest value was always found for the *U* band.

Among the eight observed carbon stars with significant linear polarization, only CZ Hya presents a polarization that increases systematically towards the ultraviolet. In general, T Dra also shows a systematical increase to the ultraviolet, but during one observing run (JD=2455000.77) it showed a drop in the ultraviolet polarization.

V Hya, R For, Y Cvn, R Lep, and RT Cap show a dip in their degree of polarization in the *V* or *B* bands. This dip has been observed previously by Raveendran (1991) for UU Aur and for SS Vir by Kruszewski et al. (1968). In all these cases, the polarization is larger in the *R* band than in the *V* or *B* bands. At low levels of polarization, distortion of the intrinsic polarization by the interstellar component could be significant. For our stars, interstellar

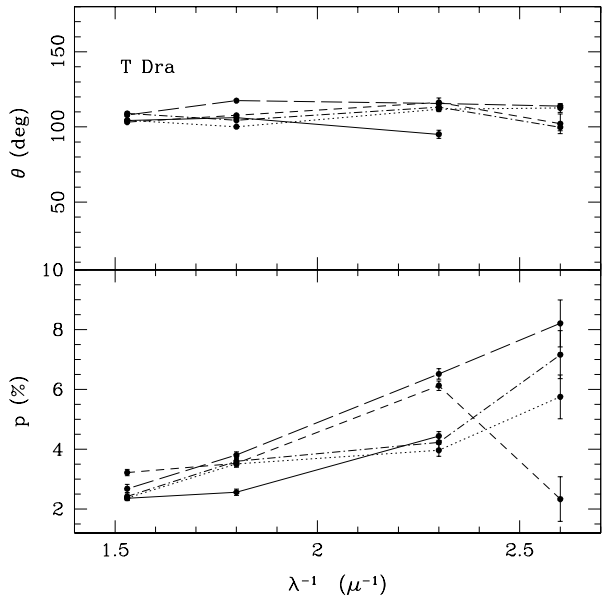

Fig. 6. Same as Figure 1, but for T Dra on JD=2454913.93 (solid line), 2454951.88 (dotted line), 2455000.77 (short-dashed line), 245503972 (long-dashed line), and 2455067.69 (dot-short-dashed line).

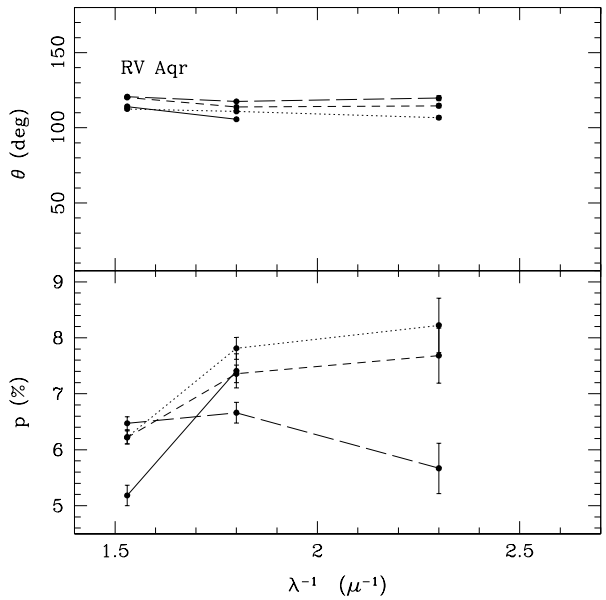

Fig. 7. Same as Figure 1, but for RV Aqr on JD=2455000.97 (solid line), 2455038.87 (dotted line), 2455096.64 (short-dashed line), and 2455126.63 (long-dashed line).

polarization was presumed to be negligible because of their high galactic latitude ($|b^{II}| \geq 20°$).

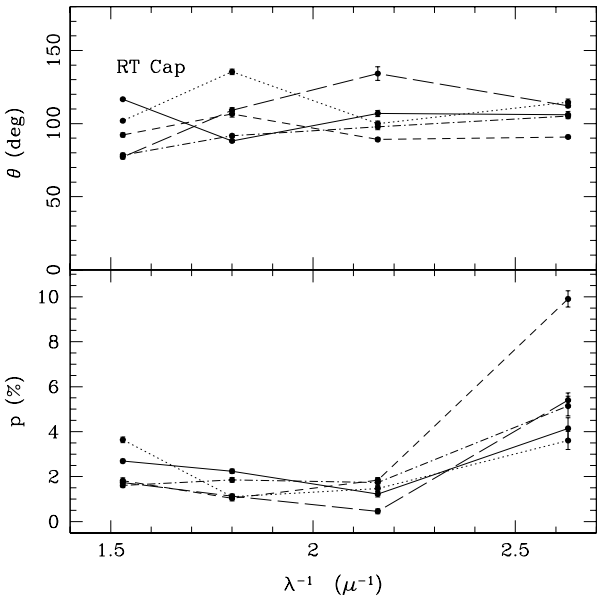

Fig. 8. Same as Figure 1, but for RT Cap on JD=2455003.90 (solid line), 2455038.85 (dotted line), 2455067.76 (short-dashed line), 2455095.63 (long-dashed line), and 2455127.58 (dot short-dashed line).

4.2. *Polarization mechanism*

Harrington (1969) has shown that light emerging from the limb of a star would be highly polarized due to Raleigh scattering by molecules or atoms, if the Planck function has a steep gradient in the atmosphere. However, for a net observable polarization, a photospheric asymmetry should be present and the proposed sources of asymmetry are non-radial pulsation of the star, variation of the temperature over the surface, and the presence of giant convection cells (Harrington 1969; Schwarzschild 1975).

Another suggested mechanism is the scattering by molecules or dust grains in an extended asymmetric circumstellar envelope (Kruszewski et al. 1968; Shawl 1975; Daniel 1978). This is the main mechanisms usually invoked to explain the intrinsic linear polarization of late-type stars in general.

4.3. *Time dependence*

The observed carbon stars show large variations of the degree of polarization and of the position angle over time. Some stars show a large swing from being highly polarized to being almost unpolarized.

T Dra and RV Aqr show an almost constant position angle during the period of observation: their spread is about 30 degrees. This suggests that the formation and destruction of dust and molecules proceeds without changes of the geometry of the inner

TABLE 3

POLARIZATION RESULTS COMPARISON

Name	Filter	p (deg)[a]	θ (deg)[a]	Reference
V Hya	U	5.7 ± 0.3	59 ± 1	This paper
	...	(1.52, 1.66)	(6, 9)	Serkowski & Shawl (2001)
	B	3.6 ± 0.1	59 ± 1	This paper
	...	(1.31, 3.14)	(173, 14)	Serkowski & Shawl (2001)
	V	2.2 ± 0.1	124 ± 1	This paper
	...	(0.68, 2.26)	(172, 13)	Serkowski & Shawl (2001)
R For	V	(0.3, 2.1)	(54,77)	This Paper
	...	1.57 ± 0.02	148	Serkowski & Shawl (2001)
R Lep	B	(0.7, 2.5)	(42,109)	This Paper
	...	(1.2, 3.00)	(37, 59)	Raveendran (2002)
	...	(0.3, 3.46)	(4, 173)	Serkowski & Shawl (2001)
	...	(1.4, 2.71)	(19, 45)	Dyck & Sandford (1971)
	...	(1.7, 1.93)	(27, 44)	Kruszewski et al. (1968)
	V	(0.8, 1.8)	(48, 134)	This Paper
	...	(1.1, 1.94)	(28, 48)	Raveendran (2002)
	...	(0.55, 2.48)	(13, 72)	Serkowski & Shawl (2001)
	...	(1.53, 1.78)	(30, 33)	Dyck & Sandford (1971)
	...	(2.15, 2.21)	(22, 32)	Kruszewski et al. (1968)
	...	2.7	25	Serkowski (1966)
	R	(1.3,2.8)	(50, 135)	This Paper
	...	(1.65, 1.75)	(16, 49)	Raveendran (2002)
Y Cvn	B	(0.2, 1.2)	(50, 138)	This Paper
	...	0.57 ± 0.37	37 ± 18	Raveendran (1991)
	...	0.25	...	Serkowski (1971)
	V	(0.5, 1.5)	(49, 98)	This Paper
	...	0.58 ± 0.04	70 ± 2	Raveendran (1991)
	R	(1.6, 1.7)	(75, 131)	This Paper
	...	0.44 ± 0.04	62 ± 3	Raveendran (1991)

[a]The range of published values are indicated in parenthesis.

regions, where most of the linear polarization is produced.

Figures 9, 10, and 11 show the brightness and polarization as a function of time for RT Cap, T Dra, and Y Cvn, respectively. In general, ultraviolet polarization shows the largest time variations in degree of polarization and position angle. In all three cases, the brightness of the star in the *UBVR* bands was almost constant.

Serkowski (1966) found that some stars exhibit a well-defined relation between light and polarization variations such that the polarization achieves the largest value at minimum light and the smallest value at maximum light. However, Zappala (1967) has concluded, based on his observations of 12 stars, that there is no correlation between luminosity and polarization changes. Clearly, more observations covering a longer time base and a closer follow-up are needed to decide whether such correlation exists.

The rather weak wavelength dependence of linear polarization indicates that circumstellar grain scattering is the main mechanism responsible for the continuum polarization in carbon stars. The identification of grains in the envelope presents a major difficulty, because of the inverse nature of the problem involved. Polarization models of circumstellar grain scattering by Raveendran (1991) show that graphite does not adequately explain the mean polarimetric behavior of carbon stars. Furthermore, graphite grains do not explain the IR spectra of the

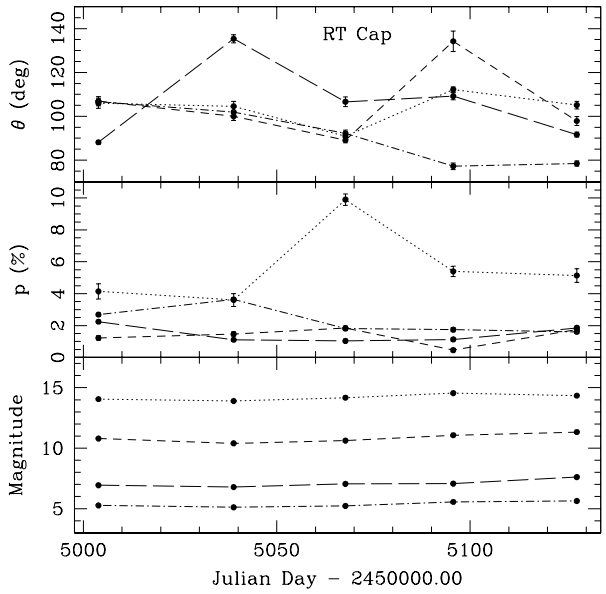

Fig. 9. RT Cap. Brightness, degree, and position angle of polarization as a function of time for U (dotted line), B (short-dashed line), V (long-dashed line), and R (dot short-dashed line) bands.

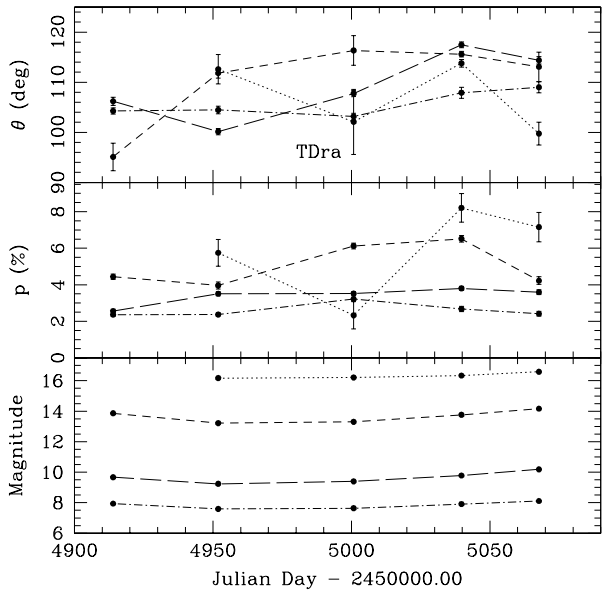

Fig. 10. Same as Figure 9, but for T Dra.

circumstellar dust envelopes around the carbon-rich objects either (Rowan-Robison & Harris 1983). It has been pointed out by Czyzak, Hirth, & Tabak (1982) that graphite formation in circumstellar envelopes is very unlikely and that carbon grains exist, most likely, in some other form, such as amorphous

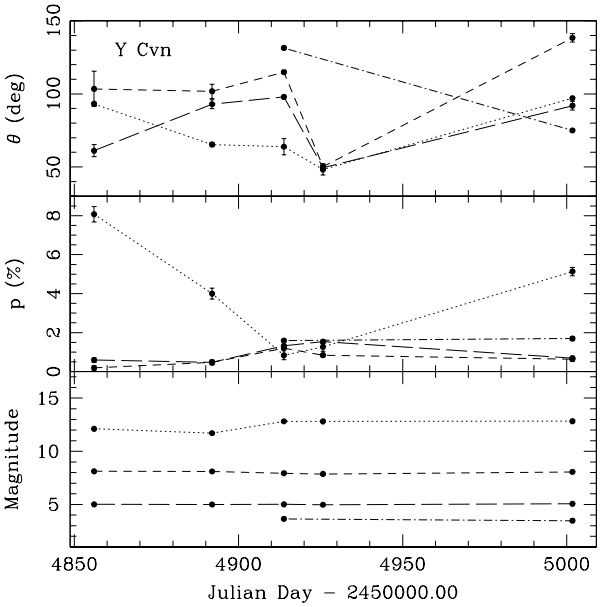

Fig. 11. Same as Figure 9, but for Y Cvn.

carbon. Dust and gas emission models for circumstellar envelopes of evolved carbon stars by Hiriart & Kwan (2000) also show that amorphous carbon grains can better reproduce the observed spectrum in these envelopes.

For Rayleigh scattering, a saturation of the amount of polarization occurs at the wavelength at which multiple scattering becomes important, and is controlled by the optical thickness of the scattering medium. Therefore, Rayleigh scattering may produce a plateau in the polarization as a function of wavelength due to the changes in the local conditions. This effect may explain the wavelength dependence of polarization for RV Aqr, which shows a plateau between the V and B bands.

5. SUMMARY

1. We have presented measurements of linear polarization for eight high-latitude carbon-rich stars in the *UBVR* bands and analyzed the polarimetric variability over time scales of months. Since the observed stars are located at high galactic latitudes, there is evidence for intrinsic linear polarization produced by their circumstellar envelopes, and negligible contribution from the interstellar medium.

2. Although the emission from evolved stars at short wavelengths is very dim, we were able to measured a quite large linear polarization from these stars in the blue and ultraviolet bands.

3. The wavelength dependence seems to be different for each star. However, a common characteristic

for all of them is the increase in the degree of linear polarization towards short wavelengths, reaching the highest values in the ultraviolet.

4. The large changes in the degree of linear polarization in the U and B bands may be explained as a result of formation and destruction processes of dust and molecules at the complex inner regions of the circumstellar envelope. Variations in the position angle may be interpreted as changes of the geometry at these inner regions produced by shock waves there.

5. The evolved stars in our study show variations in the degree of polarization over different time scales and these variations do not seem to be related to the photometric period.

The authors are very grateful to the staff of the OAN-SPM during several observing runs. J. M. López thanks to Conacyt for a graduate student fellowship. We thank Jorge Valdéz, Fernando Quirós, Benjamín García, and Esteban Luna for their contributions to the design and construction of POLIMA.

REFERENCES

Czyzak, S. J., Hirth, J. P., & Tabak, R. G. 1982, Vistas Astron., 25, 337
Daniel, J. Y. 1978, A&A, 67, 345
Dyck, H. M., & Sandford, M. T. 1971, AJ, 76, 43
Habing, H. J., te Lintel Hekkert, P., & van der Veen, W. E. C. J. 1989, in IAU Symp. 131, Planetary Nebulae, ed. S. Torres-Peimbert (Dordrecht: Kluwer), 359
Harrington, J. P. 1969, Astrophys. Lett., 3, 165
Hiriart, D. 1998, PhD Thesis, Univ. of Massachusetts, USA
Hiriart, D., & Kwan, J. 2000, ApJ, 532, 1006
Hiriart, D., Valdez, J., Quiros, F., García, B., & Luna, E. 2005, POLIMA Manual de Usuario, MU-2005-08 (México: Instituto de Astronomía, Universidad Nacional Autónoma de México)
Johnson, J., & Jones, T. 1991, AJ, 101, 1735
Kahn, F. D., & West, K. A. 1985, MNRAS, 212, 837
Kruszewski, A., Gehrels, T., & Serkowski, K. 1968, AJ, 73, 677
Landolt, A. U. 1992, AJ, 104, 340
Oloffson, H., Eriksson, K., Gustafsson, B., & Carlström, U. 1993, ApJS, 87, 267
Raveendran, A. V. 1991, A&A, 243, 453
_____. 2002, MNRAS, 336, 992
Raveendran, A. V., & Kameswara Rao, N. 1989, A&A, 215, 63
Rowan-Robison, M., & Harris, S. 1983, MNRAS, 202, 797
Schmidt, G. D., Elston, R., & Lupie, O. L. 1992, AJ, 104, 1563
Schwarzschild, M. 1975, ApJ, 195, 137
Serkowski, K. 1966, ApJ, 144, 857
_____. 1971, Kitt Peak Obs. Contr., 554, 107
Serkowski, K., & Shawl, S. J. 2001, AJ, 122, 2017
Shawl, S. J. 1975, AJ, 80, 602
Trammell, S., Dinerstein, H., & Goodrich, R. 1994, AJ, 108, 984
Zappala, R. R. 1967, ApJ, 148, L81

José Manuel López and David Hiriart: Instituto de Astronomía, Universidad Nacional Autónoma de México, Apdo. Postal 877, 22830 Ensenada, B. C., Mexico (jmlopez, hiriart@astrosen.unam.mx).